

# A PARALLACTIC DISTANCE OF $389_{-21}^{+24}$ PARSECS TO THE ORION NEBULA CLUSTER FROM VERY LONG BASELINE ARRAY OBSERVATIONS

KARIN M. SANDSTROM, J. E. G. PEEK, GEOFFREY C. BOWER, ALBERTO D. BOLATTO AND RICHARD L. PLAMBECK  
Department of Astronomy and Radio Astronomy Laboratory, University of California at Berkeley, Berkeley, CA 94720

ACCEPTED TO APJ: June 15, 2007

## ABSTRACT

We determine the parallax and proper motion of the flaring, non-thermal radio star GMR A, a member of the Orion Nebula Cluster, using Very Long Baseline Array observations. Based on the parallax, we measure a distance of  $389_{-21}^{+24}$  parsecs to the source. Our measurement places the Orion Nebula Cluster considerably closer than the canonical distance of  $480 \pm 80$  parsecs determined by Genzel et al. (1981). A change of this magnitude in distance lowers the luminosities of the stars in the cluster by a factor of  $\sim 1.5$ . We briefly discuss two effects of this change—an increase in the age spread of the pre-main sequence stars and better agreement between the zero-age main-sequence and the temperatures and luminosities of massive stars.

*Subject headings:* astrometry — stars: distances — stars: individual (GMR A) — open clusters and associations: individual (Orion Nebula Cluster) — techniques: interferometric

## 1. INTRODUCTION

The Orion Nebula is the nearest example of ongoing massive star formation. As such, it has an important place in our understanding of this fundamental process. Observations of luminosities, masses and linear scales in the Orion Nebula all depend on the distance to the cluster. For many years, the most often used distance measurement to Orion has been  $480 \pm 80$  parsecs, as determined by Genzel et al. (1981). The Hipparcos mission was only able to marginally detect the parallax of one star in the cluster, resulting in a distance of  $361_{-87}^{+168}$  pc. Other techniques of estimating the distance to the cluster provide values with large uncertainties and systematic errors, but which are generally consistent within the Genzel et al. range.

At the canonical distance of 480 parsecs, the annual parallax of an object in the Orion Nebula would be about 2 milli-arcseconds. In order to measure this parallax to high precision, angular resolution far in excess of 1 milli-arcsecond is necessary. The Very Long Baseline Array (VLBA) can achieve this degree of angular resolution, and it has thus been a very useful tool for determining parallaxes for radio sources out to a few kpc (e.g. Brisken et al. (2002); Chatterjee et al. (2004); Hachisuka et al. (2006); Loinard et al. (2005)).

In order to obtain a precise measurement of the distance to Orion using VLBI, the target source must be compact and persistent. A number of compact radio sources have been observed in Orion, first by Garay et al. (1987) and later by Felli et al. (1993a) and others. At least ten of the sources detected by these authors were identified as nonthermal radio stars because of their compactness (unresolved by the VLA A-array) and variability (Felli et al. 1993b). Bower et al. (2003) observed one of these sources, GMR A, over the course of an extreme millimeter flaring event, during which its 86 GHz flux density increased by a factor of 5 over a few hours. Follow-up observations with the VLBA detected GMR A at 15 and 22 GHz with a compact size of less than

1 milli-arcsecond. We obtained five additional epochs of VLBA observations spaced over the following year to monitor the astrometric motion of the source. We detect GMR A in four of those five observations, indicating that this source was persistent enough to allow measurement of its proper motion and parallax, thus determining the distance to Orion in a model-independent manner.

Unlike other published distance measurements to Orion, the parallactic distance presented here is model-independent. Genzel et al. (1981) determined a distance of  $480 \pm 80$  pc by modeling the proper motions and radial velocities of H<sub>2</sub>O masers in the BN/KL region with an expanding, thick shell—a technique which required assumptions about the geometry of the system of masers. Most other available distance measurements to Orion rely on stellar models in some way. Because the maser distance is independent of stellar properties it has become the canonical distance to Orion. Recently, Jeffries (2007) have found a distance of  $392 \pm 32$  pc based on the statistical properties of rotation in pre-main sequence stars. In determining this distance, Jeffries (2007) assume a spectral type - effective temperature scale for pre-main sequence stars and a random distribution of spin axes. In addition, they also must accurately identify stars which are still in the accretion phase of their pre-main sequence lifetime. Parallax provides a fundamental measure of the distance, avoiding the systematic uncertainties associated with these other techniques.

Accurate knowledge of the distance to the Orion Nebula Cluster is important for the general understanding of star-formation in the region. Luminosities are proportional to distance squared and the ages of pre-main sequence stars are typically determined by comparing their temperatures and luminosities with theoretical models (for example, Palla & Stahler (1999)). Changes in the luminosity of the stars translate directly into changes in their inferred ages, and the age distribution of the pre-main sequence stars in the cluster is a key component of any model which attempts to explain the mode of star-formation in the region.

In Section 2.1 we describe the VLBA observations and

in Section 2.2 we discuss their reduction. In particular we discuss the use of a dual calibrator method developed by Fomalont (2005). Section 3 covers the analysis of our positions for the source and presents our best fit values for the parallax and proper motion. In Section 4 we discuss how this measurement will affect the study of the Orion Nebula and its star-formation and compare our measurement with previous results.

## 2. OBSERVATIONS AND DATA REDUCTION

### 2.1. VLBA Observations

The observations were carried out at a frequency of 15 GHz with all available VLBA antennas. There were six epochs of VLBA observations: an initial observation of the source in January of 2003 in the wake of its flaring event and five epochs evenly spaced over one year to adequately sample the entire parallactic ellipse of GMR A.

To determine the astrometric position of GMR A, we use phase-referencing to the bright quasar J0541–0541 which is located 1.6 degrees to the southeast of the target. Additionally, to account for phase variation due to atmospheric gradients between J0541–0541 and GMR A, we observe a secondary calibrator J0529–0519 which is 1.3 degrees northwest of GMR A and approximately colinear with GMR A and J0541–0541. The data reduction utilizing these two calibrators in the phase-referencing is described in the following section. Each observation, excluding January 2003, consisted of alternating 40 second integrations on the two calibrator sources and on GMR A for 6 hours. The first epoch, January 2003, was part of a campaign to understand the millimeter and x-ray flare from GMR A at high resolution. The secondary calibrator was not included in this track, which consisted of alternating observations of only GMR A and J0541–0541 for 40 seconds each. A very bright calibrator, J0530+1331, was observed a few times during the course of each track for use in removing instrumental phase offsets and delays in each IF.

### 2.2. Data Reduction

The data reduction was performed in AIPS. The initial calibrations proceeded as described in the AIPS cookbook for VLBA data reduction. These include amplitude calibration and fringe-fitting to determine the instrumental single-band delay (slope of phase vs. frequency introduced by the instrument) and the residual phase delays and rates introduced by the atmosphere and inaccuracies in the correlator model.

Recently discovered errors in the Earth Orientation Parameters (EOPS) used by the VLBA correlator for all epochs excluding January 2003 were corrected using the task CLCOR as described in the VLBA Memo 69<sup>1</sup>. The data were corrected for the single- and multi-band delays with the task FRING. The target source is detected at 5- $\sigma$  or greater, in four out of the six epochs using only phase-referencing to the main calibrator J0541–0541. In the October 2004 observation, GMR A is only detected after ATMCA correction as described below. In April 2004, there are a number of significant peaks in the image because the flux from GMR A has been scattered

by poor phase coherence, probably due to fluctuations in tropospheric water vapor. We have omitted the April 2004 data from the following analysis because of its poor quality.

In order to improve the image quality and remove some systematic errors in the position of the target source we used dual-source phase-referencing as implemented in the AIPS task ATMCA (Fomalont 2005). This corrects for phase gradients across the sky due to tropospheric effects. The correction can be done in a number of ways, but in our case we used interpolation between two calibrator sources placed on either side of the target. Prior to ATMCA we also correct for the effects of structure in our calibrators through self-calibration cycles on both sources. It is clear from the images that both calibrators have resolved structure, which makes the self-calibration cycle important for accurate imaging of the target source. We note that the structure of the main calibrator appears to be approximately constant over the time period of our observations. We see at most a few percent variation in the brightness distribution of J0541–0541 comparing between epochs with clean components all restored to the lowest resolution of the five observations. Because of the lack of variation in the source structure and the high signal-to-noise of the calibrator observations, the self-calibration cycle should be sufficient to correct systematic errors in the phase solutions due to the structure of the calibrator. After ATMCA calibration we see an increase in the compactness of GMR A of up to 17 percent. Additionally, in the October dataset, the significance of the GMR A detection changes from  $< 4$  to 5 sigma. The effects of the dual-source calibration are summarized in Table 3.

After ATMCA, cleaned images of the sources were made using the task IMAGR. In each epoch, we measured the position of GMR A with reference to the main calibration source J0541–0541 for which we assume the J2000.00 position R.A.  $5^{\text{h}}41^{\text{m}}38^{\text{s}}084106$ , Dec.  $-5^{\circ}41'49''42841$ . The position assumed for the secondary calibrator, J0529–0519 in J2000.00 is R.A.  $5^{\text{h}}29^{\text{m}}53^{\text{s}}532715$ , Dec.  $-5^{\circ}19'41''61564$ . This position is used in the course of ATMCA calibration. The five images of GMR A are shown in Figure 1, centered on the maximum point in each image. The images of the calibrators J0541–0541 and J0529–0519 are shown in Figures 2 and 3, respectively. In these figures the positions are relative to the maximum of the image in the December 2003 observation.

It is clear from the integrated flux densities listed in Table 1 that we observe significant variability in GMR A at 15 GHz. This observation is in line with previous studies that show large changes in the source flux density (Felli et al. 1993b; Zapata et al. 2004; Bower et al. 2003). Bower et al. (2003) postulate that the structure of GMR A consists of a compact, highly variable source that the VLBA detects and an extended,  $\sim 5$  mJy envelope that is resolved out. Our observations certainly indicate that the source detected by the VLBA is highly variable.

#### 2.2.1. Structure in the VLBI Images of GMR A

The images of GMR A shown in Figure 1 show resolved structure. At the distance we measure to the cluster, stellar photospheres should be unresolved. We can estimate the photospheric radius of GMR A from

<sup>1</sup> VLBA Test Memo 69, October 6, 2005  
<http://www.vlba.nrao.edu/memos/test/test69memo/index.html>

TABLE 1  
GMR A POSITIONS AND FLUXES

Date	R.A. (J2000)	R.A. Error ( $\mu$ as)	Dec. (J2000)	Dec. Error ( $\mu$ as)	Noise Level (mJy/beam)	Int. Flux Density (mJy)
29 Jan 2003	5 35 11.80269059	14.84	-5 21 49.246612	36.48	0.395	11.366 $\pm$ 0.785
22 Dec 2003	5 35 11.80289569	29.89	-5 21 49.247830	93.57	0.267	6.815 $\pm$ 0.875
12 Jun 2004	5 35 11.80297711	36.82	-5 21 49.246546	86.22	0.280	4.217 $\pm$ 0.743
15 Oct 2004	5 35 11.80317743	50.88	-5 21 49.249019	163.29	0.271	2.791 $\pm$ 0.731
11 Dec 2004	5 35 11.80305485	11.47	-5 21 49.249859	21.66	0.321	23.002 $\pm$ 0.974

NOTE. — Positions measured relative to the assumed J2000.00 position of J0541-0541, R.A.  $5^{\text{h}}41^{\text{m}}38^{\text{s}}.084106$ , Dec.  $-5^{\circ}41'49''.42841$ . The errors listed are the formal errors from Gaussian fitting.

TABLE 2  
J0529-0519 POSITIONS AND FLUXES

Date	R.A. (J2000)	R.A. Error ( $\mu$ as)	Dec. (J2000)	Dec. Error ( $\mu$ as)	Noise Level (mJy/beam)	Int. Flux Density (mJy)
29 Jan 2003	...	...	...	...	...	...
22 Dec 2003	5 29 53.53352197	2.867	-5 19 41.616801	8.036	2.042	178.80 $\pm$ 3.09
12 Jun 2004	5 29 53.53351859	4.541	-5 19 41.616825	10.928	2.415	120.91 $\pm$ 4.60
15 Oct 2004	5 29 53.53351577	3.804	-5 19 41.616909	9.789	2.863	142.64 $\pm$ 4.27
11 Dec 2004	5 29 53.53351540	4.153	-5 19 41.616692	8.757	2.399	174.45 $\pm$ 3.70

NOTE. — Positions measured relative to the assumed J2000.00 position of J0541-0541, R.A.  $5^{\text{h}}41^{\text{m}}38^{\text{s}}.084106$ , Dec.  $-5^{\circ}41'49''.42841$ . The errors listed are the formal errors from Gaussian fitting.

TABLE 3  
EFFECTS OF ATMCA CALIBRATION

Date	$\Delta_{\text{R.A.}}$ ( $\mu$ as)	$\Delta_{\text{Dec}}$ ( $\mu$ as)	Total Shift ( $\mu$ as)	% Change Area <sup>a</sup>	% Change Peak Flux <sup>b</sup>
29 Jan 2003	...	...	...	...	...
22 Dec 2003	-4.36	115.92	116.02	-13.2	+20.6
12 Jun 2004	-84.60	88.92	122.46	-17.4	-15.9
15 Oct 2004	...	...	...	...	...
11 Dec 2004	+85.32	83.16	119.14	-11.5	+24.1

<sup>a</sup>The area of the source is defined here as  $\pi ab$  where the  $a$  and  $b$  values are the FWHM of the major and minor axes of the best fit Gaussian.

<sup>b</sup>The peak flux is measured in units of Jy/beam.

the bolometric luminosity of  $6 L_{\odot}$  and the spectral type K5 V as determined by Bower et al. (2003), given the effective temperature - spectral type calibration for pre-main sequence stars of Cohen & Kuhi (1979). This yields a radius of  $\sim 4.3 R_{\odot}$ , which at the distance of Orion is  $\sim 50 \mu\text{as}$ , well below the resolution of our observations. Since there is resolved structure present in the images, we must consider its source in determining the position of GMR A. Scattering by turbulent interstellar plasma can cause angular broadening. We estimate the effects of interstellar scattering on our images using the Cordes & Lazio (2002) model, which predicts an angular broadening scale at 15 GHz of  $\sim 3 \mu\text{as}$  for the line of sight to the calibrators and  $\sim 0.05 \mu\text{as}$  for GMR A. The measured size of our calibrators are consistent with very little or no interstellar scattering, in agreement with the model predictions. Some of the structure in our images is most likely due to atmospheric calibration errors. In particular, the correction from ATMCA applies mostly in the Right Ascension dimension due to the positioning of our two calibrator sources East-West relative to GMR A. It is the case that most of the images are elongated more in the Declination dimension compared to the beam shape, suggesting atmospheric effects.

However, there is also more persistent structure, mainly obvious when GMR A is bright. Bower et al. (2003) noted this structure and found that the January 2003 observation could be equally well represented by a Gaussian extended relative to the beam shape or by two unresolved sources with a separation of 0.8 mas. In the December 2003 and 2004 observations as well, we see structures that are better represented by two unresolved sources or an extended Gaussian. We considered the possibility of binarity to explain the resolved structure and we note that if GMR A were a binary, orbital motion would introduce scatter into our solution for the parallax and proper motion. Using the positions determined by fitting two unresolved sources to the images, we attempted to find a mass ratio which gave a center of mass position between the two purported sources that decreased the scatter in the parallax and proper motion solution. Because there is no consistent way to distinguish between the two sources, we also searched through the 16 possible permutations of primary and secondary components. For each of these permutations, we also attempted to fit a relative visual binary orbit using a technique based on that of Hartkopf et al. (1989). We were unable to find a consistent solution that improved

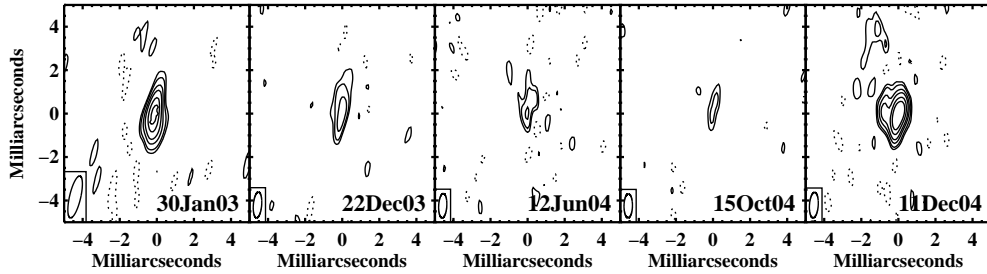


FIG. 1.— Images of GMR A for all epochs. All images are after ATMCA calibration, except for the January 2003 image, as described in the text. Each image is centered on the brightest pixel of that image. The contour levels are -2.5, 2.5, 4, 7, 10, 15 and 20 times the noise level of the individual image. The dotted contours are the negative values. The noise levels are listed in Table 1. The synthesized beam is shown in the lower left corner.

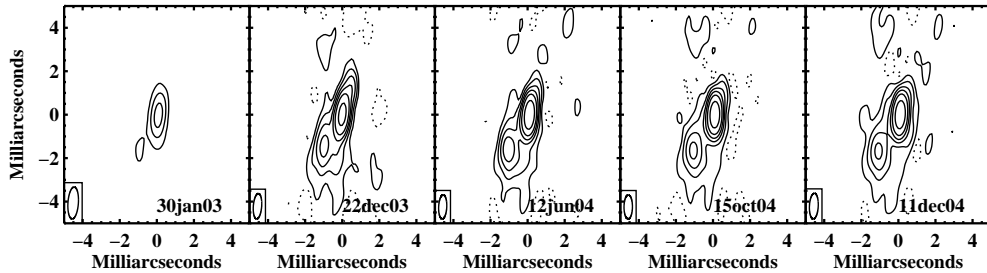


FIG. 2.— Images of the primary calibrator at each epoch with ATMCA calibration, except for the January 2003 observation which does not have ATMCA calibration but has been through an amplitude and phase self-calibration cycle. The images are centered on the location of the brightest pixel in the December 2003 image. The contour levels are -5, 5, 20, 50, 100, 200, 500 times the noise level of the individual image. The synthesized beam is shown in the lower left of each image. Negative contours are shown with dotted lines. In the January 2003 image there are no pixels less than -5 times the noise level.

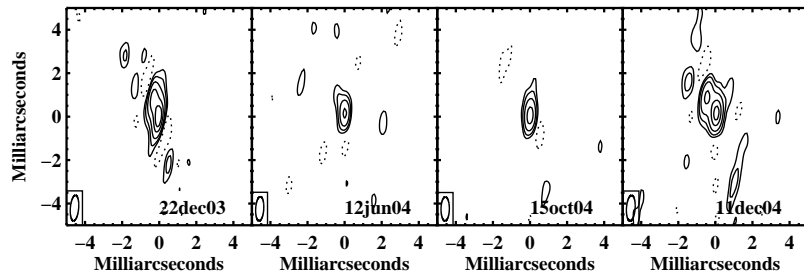


FIG. 3.— Images of the secondary calibrator, with ATMCA calibration. The images are centered on the location of the brightest pixel in the December 2003 image. The contours are -5, 5, 10, 20, 40 and 60 times the noise level of the individual image. The synthesized beam is shown in the lower left of each image. Negative contours are shown with dotted lines.

the scatter of our parallax and proper motion using these two complementary techniques. Therefore, it seems unlikely that the structure in our images is due to a binary companion.

A more likely explanation for the structure in our images is large scale magnetic features associated with the star. These have been observed with VLBI in other magnetically active weak-line T Tauri stars (Phillips et al. 1991; Andre et al. 1992) with sizes of up to 10-20  $R_*$ . A separation of 0.8 mas at the distance we measure to Orion corresponds to  $\sim 15 R_*$ , which is comparable to structures observed on other weak-line T Tauri stars. We do know that GMR A has a  $\sim 2$  kG photospheric magnetic field (Bower et al. 2003) and experiences a high level of magnetic flaring activity as seen in x-ray, millimeter and radio observations, so it seems reasonable to expect large scale magnetic structures around the star. The effect of the positional jitter introduced in our measurements by imperfectly calibrated atmosphere and by source structure is to increase the error bars in the distance determination.

### 2.2.2. Astrometric Positions of GMR A

If GMR A were unresolved and we could account for the effects of the atmosphere by observing a known point source, the best technique for determining the positions of the target would be to fit a fixed-size Gaussian to the images. The size of the Gaussian would take into account the blurring effects of the atmosphere. However, since GMR A appears to have resolved structure which may vary with time and neither of our calibrators are unresolved, the best technique for determining the source positions is to fit variable size Gaussians to the images. We did this using the AIPS task JMFIT, allowing the dimensions and position angle of the fit Gaussian to vary. Table 4 lists the dimensions of the beam for each observation and the properties of the best fit Gaussian. The positions derived from these fits are listed in Table 1. As a check, we have also fit the images with a Gaussian constrained to have the shape and size of the beam. The positions we find from these two techniques are consistent within their error bars, however the positions we determine from fitting the constrained Gaussian have smaller error bars, increasing the  $\chi^2$  of our parallax and proper motion solution, though it yields the same distance.

In the case of the January 2003 observation, ATMCA can not be applied, as only one calibrator was observed. To account for any systematic differences in the positions determined with and without ATMCA, we increased the uncertainty of the January 2003 observation by adding the r.m.s. effect of ATMCA on the other three observations in quadrature with its observed position errors (85  $\mu\text{as}$  in R.A. and 18  $\mu\text{as}$  in Dec.).

## 3. ASTROMETRIC ANALYSIS

The position of GMR A as a function of time is determined by its position, parallax and proper motion in the following way:

$$\alpha(t) = \alpha_0 + \mu_\alpha t + \pi f_\alpha(\alpha, \delta, t) \quad (1)$$

$$\delta(t) = \delta_0 + \mu_\delta t + \pi f_\delta(\alpha, \delta, t) \quad (2)$$

Here  $\mu_\alpha$  and  $\mu_\delta$  are the proper motions in Right Ascension and Declination, respectively, and  $\pi$  is the parallax.

$f_\alpha$  and  $f_\delta$  are the parallactic displacements for a source at a distance of 1 pc at the position of GMR A. The parallactic displacements are calculated based on the formulae presented in the U.S. Naval Observatory Almanac.

To fit to these five positions (ten data points) we employed a  $\chi^2$  fit to five parameters: position in R.A. and Dec, proper motion in R.A. and Dec., and parallax. The best fit solution had a reduced  $\chi^2$  value of  $\chi_R^2 = 10.2$ . This indicates that our error bars on the position are approximately  $\chi_R = 3.2$  times larger than the formal errors from Gaussian fitting, mostly due to systematic effects from tropospheric variations and variability of the source structure. To determine the error bars on the best fit parallax and proper motion we proceeded in the following way: first, we added systematic errors in quadrature to the error bars listed in Table 1 to achieve  $\chi_R^2 = 1$ ; we then did a Monte Carlo simulation in which we added offsets, drawn from a Gaussian distribution centered at zero with a width representing the total positional errors from the previous step, to the measured positions and fit for the astrometric parameters. The resulting distributions of parallax and proper motion were well-represented by Gaussians, allowing a straightforward determination of the 1- $\sigma$  errors.

The best approach to adding in systematic errors to achieve  $\chi_R^2 = 1$  is not well-defined, so we approach the problem with a few different techniques. To start, we added in quadrature the same systematic error in the R.A. and Dec dimensions till we reached  $\chi_R^2 = 1$ . This gave a parallax of  $2.53 \pm 0.18$  mas (equivalent to a distance of  $395_{-26}^{+30}$  pc). However, it is most likely not the case that the systematic errors are the same in R.A. and Dec. We know that our correction from ATMCA mostly applies in the Right Ascension dimension, due to the positioning of our calibrators East-West relative to the target. To address the non-uniformity of the systematic errors we added in quadrature error ellipses with varying axial ratios and determined the axial ratio for which the total area of the systematic error ellipse necessary to achieve  $\chi_R^2 = 1$  was smallest. As expected based on the positions of our calibrator sources, the necessary systematic error ellipse is larger in the Declination dimension by a factor of 2.5. To reach  $\chi_R^2 = 1$  the geometric mean of the axes of the error ellipse with these dimensions was 0.17 mas. This more realistic appraisal of our systematic errors gives a parallax of  $2.57 \pm 0.15$  mas ( $389_{-21}^{+24}$  pc). It is also possible that the systematic errors are epoch dependent. In this situation it is not clear how best to add in systematic errors unless we base them on the beam shape or the errors from Gaussian fitting (which are proportional to each other in theory,  $\sigma \sim 0.5 \frac{\theta_{\text{FWHM}}}{\text{SNR}}$ ). To explore this possibility we have scaled up the error ellipses from Gaussian fitting to achieve  $\chi_R^2 = 1$ . This technique gives a parallax of  $2.61 \pm 0.14$  mas ( $383_{-20}^{+22}$  pc), consistent with the other techniques.

We note that the astrometric parameters obtained through these various techniques are robust to our treatment of the errors. We consider adding the fixed axial ratio error ellipse to be the most realistic appraisal of the systematic errors given the positioning of the calibrators. This technique yields a parallax of  $\pi = 2.57 \pm 0.15$  mas, which corresponds to a distance of  $389_{-21}^{+24}$  pc. The proper motions of GMR A in R.A. and Dec. from this solution

TABLE 4  
BEAM SIZES AND BEST-FIT GAUSSIAN DIMENSIONS

Date	Beam FWHM (mas $\times$ mas)	Beam P. A. ( $^{\circ}$ )	Gaussian FWHM (mas $\times$ mas)	Gaussian P. A. ( $^{\circ}$ )
29 Jan 2003	$1.994 \times 0.597$	-15.52	$2.028 \times 0.738$	-10.00
22 Dec 2003	$1.195 \times 0.448$	-5.58	$2.230 \times 0.619$	-9.52
12 Jun 2004	$1.122 \times 0.438$	-3.63	$1.682 \times 0.576$	-14.13
15 Oct 2004	$1.111 \times 0.455$	-1.04	$2.114 \times 0.482$	-11.81
11 Dec 2004	$1.178 \times 0.473$	-4.53	$1.662 \times 0.800$	-12.18

are  $\mu_{\alpha} \cos \delta = 1.89 \pm 0.12$  mas yr $^{-1}$  and  $\mu_{\delta} = -1.67 \pm 0.19$  mas yr $^{-1}$ . At the distance we measure, the transverse velocity is  $v_t = 4.65 \pm 0.39$  km s $^{-1}$ . Figure 4 shows a plot of our solution and Table 5 lists the measured astrometric parameters and their uncertainties.

#### 4. DISCUSSION

The Orion Nebula is part of a very large and very complex star-formation region (see Genzel & Stutzki (1989) for a review of the large scale structure). The implications of a measurement of the distance to one star thus depend sensitively on where that star is located relative to the stellar associations and molecular gas in this region. The available evidence very strongly constrains GMR A to be a part of the Orion Nebula Cluster, located within a few parsecs of the Trapezium stars but embedded in the molecular cloud which is currently being disrupted by the ionizing radiation from  $\Theta^1$  Ori C. In the following paragraphs we will present the evidence for placing GMR A in the Orion Nebula Cluster and then proceed to compare our distance to previous measurements and, finally, briefly discuss some of the implications our distance measurement has for the general study of this important region.

##### 4.1. The Membership of GMR A in the Orion Nebula Cluster

Bower et al. (2003) observed GMR A, following its intense outburst detected with the BIMA interferometer, in the near-IR with NIRC and NIRCSPEC on the Keck telescopes. While there is no optical source coincident with the position of GMR A, there is an infrared source which they identify as a weak-line T Tauri star embedded in molecular gas. GMR A was also detected in the COUP survey as a highly variable x-ray source (COUP J053551.8–052149) (Feigelson et al. 2002; Getman et al. 2003) behind a gas column density of  $N_{\text{H}} = 10^{22.3}$  cm $^{-2}$ . The combination of the spectral classification as a K5 V star and a bolometric luminosity of  $6 L_{\odot}$  (Bower et al. 2003) suggests a very young age for this star (around 1 Myr, based on the pre-main sequence tracks of Palla & Stahler (1999)) as does its location embedded in molecular gas.

The molecular gas in Orion A, located behind the H II region created by the Trapezium stars, has a very high column depth  $A_V \approx 50 - 100$  mag, essentially providing a wall behind which no background sources are detected. Near-IR surveys have shown that the projected spatial distribution of optically visible and extincted, near-IR sources are very similar (Hillenbrand & Hartmann 1998) and that around 50% of sources are only visible in the infrared. The three-dimensional distribution of the Orion Nebula Cluster has thus been interpreted as fairly spherical with about half of that sphere still embedded in the

molecular cloud out of which it formed (Hillenbrand & Hartmann 1998). The projected distribution of stars has a radius of  $\sim 3$  pc around  $\Theta^1$  Ori C. GMR A is located 1.95 arcminutes away from the center of the cluster, which corresponds to a projected distance of 0.22 parsecs at our measured distance to the cluster. The x-ray absorption column density measured to GMR A indicates that it must be embedded in the molecular gas, but it cannot be more than a few parsecs deep. The lack of foreground and background star-forming regions, the proximity of GMR A to the Trapezium on the sky, the fact that it is embedded in molecular gas, and its very young age convincingly place GMR A as a member of the Orion Nebula Cluster.

In addressing the membership of a stellar cluster, a typical technique is to compare the velocity of a star to the average velocity and dispersion of the cluster. There have been a number of measurements of these quantities for the ONC with proper motion and radial velocity studies. Recent spectroscopic observations of stars in the cluster by Sicilia-Aguilar et al. (2005) show a mean heliocentric velocity of 25 km s $^{-1}$ , with a  $\sim 2$  km s $^{-1}$  uncertainty in the zero point and a dispersion of  $\sigma = 2.3$  km s $^{-1}$ . Bower et al. (2003) measured a heliocentric radial velocity of  $14 \pm 5$  km s $^{-1}$  for GMR A. Given the combined uncertainties in these measurements and the cluster radial velocity dispersion, GMR A is consistent with the radial velocity of the cluster.

Most proper motion studies of clusters, including that of Jones & Walker (1988) which surveyed nearly 1000 stars in Orion, measure relative proper motions. In order to compare our measurement, which is an absolute proper motion, to the results of these studies, we must first find the absolute proper motion of the ONC to subtract from our values. This value has been measured by a number of authors using different astrometric catalogs. Baumgardt et al. (2000) use the Hipparcos catalog and measure a mean proper motion of  $\mu_{\alpha} \cos(\delta) = 1.73 \pm 0.40$  mas yr $^{-1}$  and  $\mu_{\delta} = -0.47 \pm 0.27$  mas yr $^{-1}$  for the ONC. Kharchenko et al. (2003) used the ASCC catalog (which contains data from Hipparcos, Tycho and the USNO catalogs) and found very similar values  $\mu_{\alpha} \cos(\delta) = 2.02 \pm 0.74$  mas yr $^{-1}$  and  $\mu_{\delta} = -0.19 \pm 0.66$  mas yr $^{-1}$ . Later, Kharchenko et al. (2005) improved their determination of the absolute proper motion with an expanded astrometric catalog and found  $\mu_{\alpha} \cos(\delta) = 1.96 \pm 0.31$  and  $\mu_{\delta} = -0.77 \pm 0.46$  mas yr $^{-1}$ . All of these values are consistent within their error bars, so we proceed in our analysis using the recent value of Kharchenko et al. (2005). We measure a proper motion for GMR A of  $\mu_{\alpha} \cos(\delta) = 1.89 \pm 0.12$  mas yr $^{-1}$  and  $\mu_{\delta} = -1.67 \pm 0.19$  mas yr $^{-1}$ . These values are quite similar to the cluster mean. We can compare the residual velocity after

TABLE 5  
GMR A ASTROMETRIC PARAMETERS\*

Parameter	Value
Fit Quantities	
Epoch	2004.25 (MJD 53095.3)
Right Ascension $\alpha_0$	$5^{\text{h}}35^{\text{m}}11^{\text{s}}.80295404$
Declination $\delta_0$	$-5^{\circ}21'49''.247452$
$\mu_{\alpha} \cos \delta$ (mas yr $^{-1}$ )	$1.89 \pm 0.12$
$\mu_{\delta}$ (mas yr $^{-1}$ )	$-1.67 \pm 0.19$
Parallax $\pi$ (mas)	$2.57 \pm 0.15$
Derived Quantities	
Distance (pc)	$389^{+24}_{-21}$
Transverse Velocity (km s $^{-1}$ )	$4.65 \pm 0.39$
Position Angle $^{\dagger}$ ( $^{\circ}$ )	$131.5 \pm 3.7$

\* All coordinates are listed in the J2000 equinox and measured in reference to the assumed position of J0541-0541:  $5^{\text{h}}41^{\text{m}}38^{\text{s}}.084106$ , Dec.  $-5^{\circ}41'49''.42841$ .

$^{\dagger}$ The position angle of the proper motion, measured from North through East.

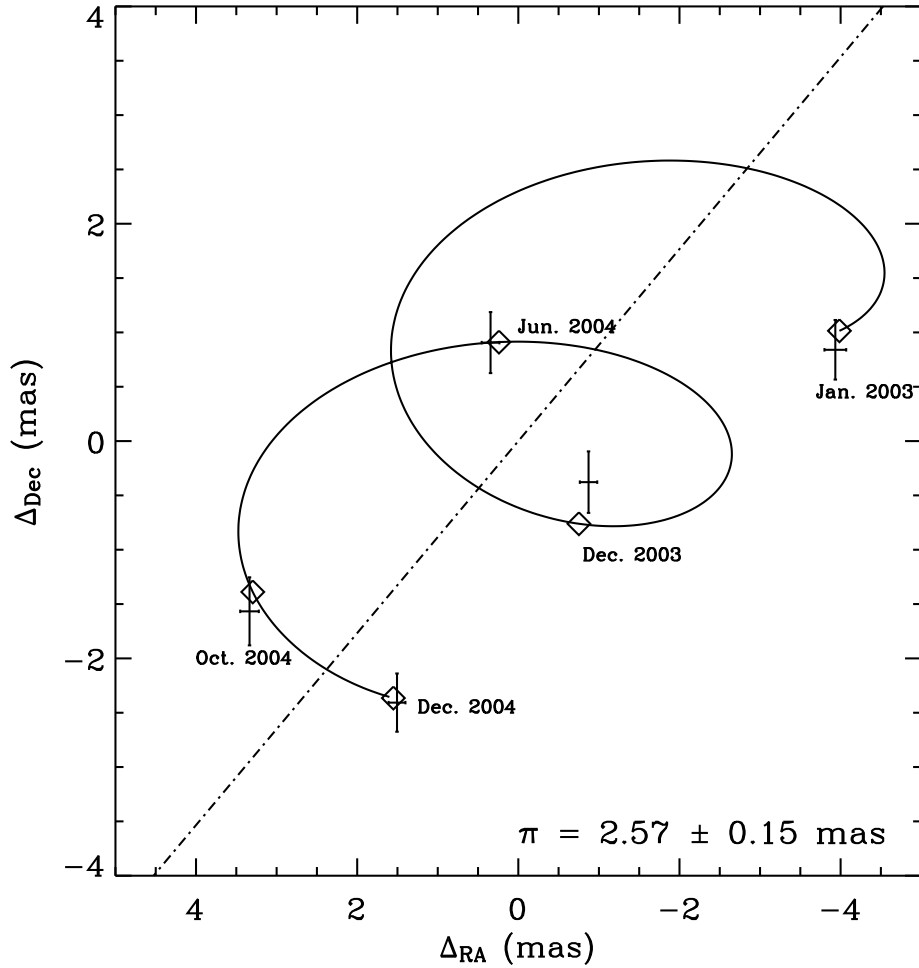


FIG. 4.— The measured positions of GMR A with the best fit parallax and proper motion. The diamonds represent the predicted position of GMR A for each observation. The error bars on the measured positions are scaled as described in the text. The dashed line is the proper motion of the source, with the parallactic motion subtracted. The parallax corresponds to a distance of  $389^{+24}_{-21}$  pc.

subtracting the mean to the velocity dispersion of the cluster. The velocity dispersion of the ONC has been measured by a number of authors. The largest survey of relative proper motions was carried out by Jones & Walker (1988). They found a one-dimensional proper motion dispersion of  $\sim 1.1 \text{ mas yr}^{-1}$  for all of the cluster stars in their survey (I magnitude of 16 or higher). Additionally, they found a trend of decreasing velocity dispersion with increasing mass (and therefore, magnitude) for stars in the ONC. Hillenbrand & Hartmann (1998) show that for stars with masses between 0.1 and  $0.3 M_{\odot}$  the dispersion is  $\langle \sigma \rangle \approx 1.26 \text{ mas yr}^{-1}$  and for stars between 1 and  $3 M_{\odot}$  it decreases to  $1.00 \text{ mas yr}^{-1}$ . The proper motion of GMR A is less than  $1\text{-}\sigma$  from the cluster average indicating a very high membership probability.

At the distance we measure to the ONC, a velocity of  $1 \text{ mas yr}^{-1}$  is equivalent to  $1.85 \text{ km s}^{-1}$ . Relative to the cluster, GMR A is moving  $0.13 \pm 0.61 \text{ km s}^{-1}$  West,  $1.67 \pm 0.93 \text{ km s}^{-1}$  South, and  $-11.0 \pm 5.4 \text{ km s}^{-1}$  along the line of sight. We note that there are large uncertainties in the radial velocity, both for GMR A and for the cluster as a whole. However, even at  $-11 \text{ km s}^{-1}$  relative to the cluster, GMR A would only have moved  $\sim 10 \text{ pc}$  over its lifetime.

There is one measurement of the proper motion of GMR A in the literature by Gomez et al. (2005). They determined the absolute proper motions of 35 radio sources in Orion with archival VLA data spanning 15 years. Although we have much higher angular resolution in our observations, their long time baseline makes the comparison useful. They measure the absolute proper motion of the cluster to be  $\mu_{\alpha} \cos(\delta) = 0.8 \pm 0.2 \text{ mas yr}^{-1}$  and  $\mu_{\delta} \cos(\delta) = -2.3 \pm 0.2 \text{ mas yr}^{-1}$ . These values are quite different from others in the literature. The absolute proper motion for GMR A they find is  $\mu_{\alpha} \cos(\delta) = -2.02 \pm 1.87 \text{ mas yr}^{-1}$  and  $\mu_{\delta} = 1.15 \pm 1.93 \text{ mas yr}^{-1}$ . Our measurement is only consistent with these values at the 2-sigma level. They find a substantially higher velocity dispersion for the cluster than found in optical surveys and theorize that the population of radio sources might have larger random velocities. However, using our proper motion, GMR A has a very typical velocity compared to the optical sources.

To summarize, GMR A is a very likely member of the Orion Nebula Cluster based on its youth, proximity to the cluster on the sky, proper motion, and location embedded in molecular gas. Having established its place in the Orion region, we now compare our distance measurement to those in the literature.

#### 4.2. Comparison with Previous Measurements

Despite its importance in our understanding of star-formation, the distance to the Orion Nebula Cluster is quite uncertain. Till recently there has only been one model-independent distance measurement—the marginally significant parallax from Hipparcos of the star HD 37061 which corresponds to a distance of  $361_{-87}^{+168}$  parsecs (Bertout et al. 1999).

Many authors have estimated the distance to the cluster by fits to the upper main sequence, a procedure which is complicated by systematic uncertainties in the models, the variable background and extinction of the Orion Nebula, and the region over which stars are included in

the analysis, among other issues. Some results with this technique are those of Penston (1973) who found a distance of  $363_{-24}^{+26}$  parsecs, using infrared photometry to characterize each star’s extinction individually; a later, more detailed analysis by Penston et al. (1975) who found  $\sim 400 \pm 20$ ; Warren & Hesser (1978) found a distance of  $483_{-51}^{+57}$  parsecs; and Anthony-Twarog (1982) who re-analyzed the data from Warren & Hesser (1978) found a distance of  $434_{-19}^{+21}$  parsecs. These results alone—some of which make use of the same data, others which use the same techniques—show a spread of more than 100 parsecs, illustrating the difficulty of such measurements. Many authors have also attempted statistical techniques which combine the proper motion and radial velocity distributions of the stars with assumptions regarding cluster expansion or contraction. Two early examples of this technique are Strand (1958) who find a distance of 525 parsecs and Johnson (1965) who find 380 parsecs.

Although the Hipparcos mission could only marginally detect the parallax of a single star in the ONC, combination of the astrometric measurements of many stars has yielded some results for Orion. Wilson et al. (2005) analyzed the aggregate astrometric motions of stars foreground and background to the Orion A in three distinct regions of the cloud. They estimate a distance of  $465_{-57}^{+75}$  parsecs to the ONC region. This distance is larger than what we measure, but is consistent with our measurement at the one-sigma level. Brown et al. (1994) also used arguments regarding foreground and background stars, but instead comparing their reddening and  $100 \mu\text{m}$  fluxes to estimate distances to the near and far edges of the cloud of 320 and 500 parsecs.

The orbital parameters of binary systems can be used in some cases to determine very accurate distances. Stassun et al. (2004) have analysed an eclipsing binary  $0.3$  degrees south of  $\Theta^1 \text{ C Ori}$  and found it to be at  $419 \pm 21$  parsecs. However, its status as a member of the ONC is somewhat uncertain because of its relatively old age and location relative to the cluster. The distance to this binary agrees with our distance to the ONC. Recent work by Kraus et al. (2007) on the visual binary system containing  $\Theta^1 \text{ Ori C}$  yields two equally good orbital solutions which their data cannot yet distinguish. Assuming a luminosity-mass relationship for the stars they find distances of  $384 \pm 11$  and  $434 \pm 12$  parsecs from the two orbits. Further astrometric and spectroscopic observations of this system may provide a very accurate distance in the future.

Genzel et al. (1981) combined observations of the proper motions and radial velocities of  $\text{H}_2\text{O}$  masers in the BN/KL region with the assumption of a spherical, uniformly expanding, thick shell and found a distance of  $480 \pm 80$  parsecs. Because of its relative precision and independence from stellar evolution calculations, this distance has become the canonical distance to the Orion Nebula Cluster. Indeed, many studies of the ONC population and star-formation make use of this distance without consideration of its substantial uncertainties. Our distance measurement is 20% closer than that of Genzel et al. (1981), though within their combined uncertainties. However, our distance is more precise and does not depend on the assumption of geometries for expanding maser sources which has been shown to be considerably



more complex in many cases than what these authors assume (Greenhill et al. 2005).

Very recently, Hirota et al. (2007) measured the annual parallax of one H<sub>2</sub>O maser spot in the Orion BN/KL outflow using VERA (VLBI Exploration of Radio Astronomy). The parallax they measure corresponds to a distance of  $437 \pm 19$  parsecs using only the motion in Right Ascension, and  $445 \pm 42$  when they solve for the parallax using both the Right Ascension and Declination. Note that these error bars are only statistical, and the latter value agrees with ours at the 1- $\sigma$  level. Parallax determinations from maser spot motion can be problematic, because of intrinsic structure changes and/or spot acceleration. For the spot in question Hirota et al. detect changes in its emission line profile over their two years of observation, which likely indicate changes in the structure of the source. Stellar parallax measurements are less vulnerable to this type of systematic uncertainty. If the difference between our VLBA measurement and the Hirota et al. VERA determination is real, and the VERA error bars are accurate, it may argue for a larger separation between the BN/KL region and the Orion Nebula Cluster along the line of sight.

Finally, we compare our distance to the recent work of Jeffries (2007) who have used the statistical properties of pre-main sequence star rotation to determine a distance of  $392 \pm 32$  parsecs to the ONC. This technique involves the assumption of random spin orientations for the stars in the cluster and makes use of a spectral type - effective temperature scale for pre-main sequence stars. From the whole sample analyzed by Jeffries (2007), a distance of  $440 \pm 34$  parsecs is derived. However, excluding stars which show evidence of accretion—a factor which makes the necessary radius determination unreliable—lowers the distance to  $392 \pm 32$  parsecs. Our distance agrees very well with this latter value. Jeffries (2007) note that the distance they determine is very sensitive to the assumed spectral type - effective temperature scale, such that distance scales with the square of the effective temperature. In addition, it is clear that the exclusion of Classical T Tauri stars, which show evidence for accretion, significantly changes the derived distance, indicating that an accurate account of the various sources of systematic error is extremely important to this technique.

To summarize, we present a distance to the ONC of  $389_{-21}^{+24}$  parsecs using the fundamental technique of parallax. In contrast to previous distance estimates, this measurement does not rely on modeling of stellar evolution, cluster dynamics, or calibrations of effective temperature for pre-main sequence stars. In comparing our measurement to previous values, we find it to be consistent with many prior measurements within their substantial error bars. We find good agreement with recent values from Jeffries (2007), Kraus et al. (2007) and Stassun et al. (2004), but independent of the various assumptions those authors are forced to make.

### 4.3. Implications of a Closer Distance to the ONC

Many studies of the Orion Nebula assume the distance of Genzel et al. (1981) or similar. Our distance is 20% closer. In luminosity terms, this change means luminosities are a factor of 1.5 lower than previously claimed, a result that is especially important for the determination

of pre-main sequence star ages, which scale with luminosity as  $t \propto L^{-3/2}$ . Therefore, at a distance of 390 parsecs, the stars are nearly twice as old as they would be at 480 parsecs. This scaling of age with luminosity is true only for fully convective pre-main sequence stars that have contracted by a substantial amount from their initial radii (see, for instance, Palla & Stahler (1999) for further discussion). Near the birthline this assumption breaks down and the ages will not be affected to the same degree. A decrease in luminosity will therefore age the entire population of pre-main sequence stars, but not uniformly, increasing the age spread of the population.

The distribution of stellar ages in Orion is the basis for many theories describing star-formation in the region and massive, clustered star-formation in general. These theories can be broken down into two general categories—those that purport that star formation in the ONC happened suddenly and quickly (e.g. Hartmann et al. (2001); Hartmann (2003)) and those that argue that star formation has been occurring over a longer timescale, but has been accelerating in recent times (e.g. Palla & Stahler (2000); Tan et al. (2006); Huff & Stahler (2006)). The age spread of cluster members is a fundamental measurement of the timescale of star-formation in the cluster. A larger age spread, as would result from the decrease in luminosity, tends to favor models where star-formation has occurred over a more extended period of time.

Another interesting feature of the stellar population in Orion is that the high mass stars seem to fall above the expected zero-age main sequence for the cluster (Palla & Stahler 1999; Hillenbrand & Hartmann 1998). Palla & Stahler (1999) argue that this must be due to a systematic problem in determining the luminosities, effective temperatures or some combination thereof. These analyses assumed a distance of 470 parsecs, so there is indeed a systematic offset—according to our measurement these luminosities are too high by a factor of 1.5. A shift of this magnitude brings the luminosities of the high mass stars into much better agreement with the zero-age main sequence predictions.

## 5. CONCLUSIONS

We have monitored the astrometric motion of the flaring, non-thermal radio star GMR A over the course of two years with the Very Long Baseline Array. We determine from these data the proper motion and parallax of the star. Based on its young age, its proximity to the center of the Trapezium on the sky, the consistency of its proper motion with that of the cluster and its location embedded in molecular gas, the probability that GMR A is a member of the Orion Nebula Cluster is very high, and thus the distance we determine based on its parallax is representative of the cluster as a whole. We find the ONC is at a distance of  $389_{-21}^{+24}$  parsecs, nearly 100 parsecs closer than the canonical distance of 480 parsecs determined by Genzel et al. (1981). The distance presented here is in good agreement with recent work by Jeffries (2007), with the advantage of being independent of assumptions about stellar properties. A closer distance has important implications for the study of star-formation in the Orion Nebula, one of the most well-studied sites of massive star formation, most notably the increase in the ages and the age spread of the pre-main sequence stars in the cluster. The decrease in luminosity also brings

the more massive stars into better agreement with the zero-age main-sequence.

Further VLBA observations of other radio stars in the ONC may overcome the limitations of a single star distance and begin to probe the depth of the cluster. In addition, suitable targets for this type of observation should be found in most clusters with substantial pre-main sequence populations. Future VLBI observations of magnetically active, pre-main sequence stars in these clusters could provide precise, fundamental distance measurements to many nearby star-forming regions.

The authors would like to thank the referee for thor-

ough and helpful comments. We would also like to thank Steve Stahler and Reinhard Genzel for sharing their expertise on the Orion region. KMS acknowledges support from an NSF Graduate Research Fellowship and would like to thank Franck Marchis and Jason Wright for helpful discussions. The research of JEGP was supported in part by NSF grant AST04-06987. The National Radio Astronomy Observatory is a facility of the National Science Foundation operated under cooperative agreement by Associated Universities, Inc.

*Facilities:* VLBA ()

#### REFERENCES

- Andre, P., Deeney, B. D., Phillips, R. B., & Lestrade, J.-F. 1992, *ApJ*, 401, 667
- Anthony-Twarog, B. J. 1982, *AJ*, 87, 1213
- Baumgardt, H., Dettbarn, C., & Wielen, R. 2000, *A&AS*, 146, 251
- Bertout, C., Robichon, N., & Arenou, F. 1999, *A&A*, 352, 574
- Bower, G. C., Plambeck, R. L., Bolatto, A., McCrady, N., Graham, J. R., de Pater, I., Liu, M. C., & Baganoff, F. K. 2003, *ApJ*, 598, 1140
- Briskin, W. F., Benson, J. M., Goss, W. M., & Thorsett, S. E. 2002, *ApJ*, 571, 906
- Brown, A. G. A., de Geus, E. J., & de Zeeuw, P. T. 1994, *A&A*, 289, 101
- Chatterjee, S., Cordes, J. M., Vlemmings, W. H. T., Arzoumanian, Z., Goss, W. M., & Lazio, T. J. W. 2004, *ApJ*, 604, 339
- Cohen, M. & Kuhl, L. V. 1979, *ApJS*, 41, 743
- Cordes, J. M. & Lazio, T. J. W. 2002, *ArXiv Astrophysics e-prints*
- Feigelson, E. D., Broos, P., Gaffney, III, J. A., Garmire, G., Hillenbrand, L. A., Pravdo, S. H., Townsley, L., & Tsuboi, Y. 2002, *ApJ*, 574, 258
- Felli, M., Churchwell, E., Wilson, T. L., & Taylor, G. B. 1993a, *A&AS*, 98, 137
- Felli, M., Taylor, G. B., Catarzi, M., Churchwell, E., & Kurtz, S. 1993b, *A&AS*, 101, 127
- Fomalont, E. B. 2005, in *ASP Conf. Ser. 340: Future Directions in High Resolution Astronomy*, ed. J. Romney & M. Reid, 460–+
- Garay, G., Moran, J. M., & Reid, M. J. 1987, *ApJ*, 314, 535
- Genzel, R., Reid, M. J., Moran, J. M., & Downes, D. 1981, *ApJ*, 244, 884
- Genzel, R. & Stutzki, J. 1989, *ARA&A*, 27, 41
- Getman, K. V., Feigelson, E. D., Garmire, G., Murray, S. S., & Harnden, Jr., F. R. 2003, *IAU Circ.*, 8068, 2
- Gomez, L., Rodriguez, L. F., Loinard, L., Lizano, S., Poveda, A., & Allen, C. 2005, *ApJ*, 635, 1166
- Greenhill, L. J., Chandler, C. J., Reid, M. J., & Humphreys, E. M. L. 2005, in *Protostars and Planets V*, 8614–+
- Hachisuka, K., Brunthaler, A., Menten, K. M., Reid, M. J., Imai, H., Hagiwara, Y., Miyoshi, M., Horiuchi, S., & Sasao, T. 2006, *ApJ*, 645, 337
- Hartkopf, W. L., McAlister, H. A., & Franz, O. G. 1989, *AJ*, 98, 1014
- Hartmann, L. 2003, *ApJ*, 585, 398
- Hartmann, L., Ballesteros-Paredes, J., & Bergin, E. A. 2001, *ApJ*, 562, 852
- Hillenbrand, L. A. & Hartmann, L. W. 1998, *ApJ*, 492, 540
- Hirota, T., Bushimata, T., Choi, Y. K., Honma, M., Imai, H., Iwadate, K., Jike, T., Kameno, S., Kameya, O., Kamohara, R., Kan-ya, Y., Kawaguchi, N., Kijima, M., Kim, M. K., Kobayashi, H., Kuji, S., Kurayama, T., Manabe, S., Maruyama, K., Matsui, M., Matsumoto, N., Miyaji, T., Nagayama, T., Nakagawa, A., Nakamura, K., Oh, C. S., Omodaka, T., Oyama, T., Sakai, S., Sasao, T., Sato, K., Sato, M., Shibata, K. M., Shintani, M., Tamura, Y., Tsushima, M., & Yamashita, K. 2007, *ArXiv e-prints*, 705
- Huff, E. M. & Stahler, S. W. 2006, *ApJ*, 644, 355
- Jeffries, R. D. 2007, *ArXiv Astrophysics e-prints*
- Johnson, H. M. 1965, *ApJ*, 142, 964
- Jones, B. F. & Walker, M. F. 1988, *AJ*, 95, 1755
- Kharchenko, N. V., Pakulyak, L. K., & Piskunov, A. E. 2003, *VizieR Online Data Catalog*, 808, 291
- Kharchenko, N. V., Piskunov, A. E., Röser, S., Schilbach, E., & Scholz, R.-D. 2005, *A&A*, 438, 1163
- Kraus, S., Balega, Y. Y., Berger, J., Hofmann, K., Millan-Gabet, R., Monnier, J. D., Ohnaka, K., Pedretti, E., Preibisch, T., Schertl, D., Schloerb, F. P., Traub, W. A., & Weigelt, G. 2007, *ArXiv Astrophysics e-prints*
- Loinard, L., Mioduszewski, A. J., Rodríguez, L. F., González, R. A., Rodríguez, M. I., & Torres, R. M. 2005, *ApJ*, 619, L179
- Palla, F. & Stahler, S. W. 1999, *ApJ*, 525, 772
- . 2000, *ApJ*, 540, 255
- Penston, M. V. 1973, *ApJ*, 183, 505
- Penston, M. V., Hunter, J. K., & Oneill, A. 1975, *MNRAS*, 171, 219
- Phillips, R. B., Lonsdale, C. J., & Feigelson, E. D. 1991, *ApJ*, 382, 261
- Sicilia-Aguilar, A., Hartmann, L. W., Szentgyorgyi, A. H., Fabricant, D. G., Fűrész, G., Roll, J., Conroy, M. A., Calvet, N., Tokarz, S., & Hernández, J. 2005, *AJ*, 129, 363
- Stassun, K. G., Mathieu, R. D., Vaz, L. P. R., Stroud, N., & Vrba, F. J. 2004, *ApJS*, 151, 357
- Strand, K. A. 1958, *ApJ*, 128, 14
- Tan, J. C., Krumholz, M. R., & McKee, C. F. 2006, *ApJ*, 641, L121
- Warren, Jr., W. H. & Hesser, J. E. 1978, *ApJS*, 36, 497
- Wilson, B. A., Dame, T. M., Mashedier, M. R. W., & Thaddeus, P. 2005, *A&A*, 430, 523
- Zapata, L. A., Rodríguez, L. F., Kurtz, S. E., & O'Dell, C. R. 2004, *AJ*, 127, 2252